ChemComm

# Nanocrystals of $CuMSnS_4$ (M = In or Ga) for Solar Energy Conversion Applications



| | |
|---|---|
| Journal: | *ChemComm* |
| Manuscript ID | CC-COM-08-2018-006644.R2 |
| Article Type: | Communication |
| | |



Journal Name

COMMUNICATION

# Nanocrystals of $CuMSnS_4$ (M = In or Ga) for Solar Energy Conversion Applications

Received 00th January 20xx,
Accepted 00th January 20xx

DOI: 10.1039/x0xx00000x

www.rsc.org/

Karthik Ramasamy,[a*] Pravin S. Shinde, [b,c] Nariman Naghibolashrafi[b] , Shanlin Pan,[b,c] and Arunava Gupta[b,c*]

**Quaternary $M^{I}M^{III}M^{IV}X_4^{VI}$ (I-III-IV-$VI_4$) chalcogenides obtained by cross-substitution of binary and ternary compounds remain relatively unexplored. We have for the first-time synthesized wurtzite and defect chalcopyrite phases of $CuMSnS_4$ (M = In or Ga) in the form of nanocrystals. Optical measurements show that the $CuMSnS_4$ (M = In or Ga) nanocrystals exhibit strong visible light absorption with band gap values between 1.15 - 1.4 eV, suitable for solar energy conversion applications.**

Meeting the growing energy demands, while addressing the carbon emission issues in the US and the world, will require effective use of a diverse renewable energy sources.[1,2] The utilization of abundant solar energy employing efficient photovoltaics (PVs) is a particularly attractive option, and has seen rapid growth.[3,4,5] The absorber material determines the effective capture and conversion of solar energy to electrical energy.[6] A wide range of materials are being explored for use as absorbers in "thin film" photovoltaics, including several that have been commercialized (CdTe, $CuIn_xGa_{1-x}S_2$) or are nearing commercialization (GaAs).[7,8,9] Regardless of production and deployment cost fluctuations, PV electricity turns out to be more expensive than any other fossil fuel source, partly because of the scarcity of absorber elements.[10,11,12] Thus, there is an active effort to develop PV absorber materials that are composed of sustainable and abundantly available elements.[13,14,15,16] As per chemical elements abundancy data, elements like Cu, Zn, Sn, Ge, Si, S, Ga, Sb are at least an order of magnitude more abundant than Te, In or As, which are the essential constituents in currently matured thin film PV technologies.[17]

In recent years, $Cu_2ZnSnS_4$ (CZTS), a direct band gap semiconductor possessing requisite optical properties and composed of abundant elements, has been investigated in detail for PV applications.[18] However, antisite disorder due to copper and zinc having similar ionic radii considerably reduces the open circuit voltage ($V_{oc}$) of CZTS-based PVs, thereby limiting the photo-conversion efficiency to 12 %.[19] On the other hand, organo-lead perovskites have quickly achieved energy conversion efficiency close to 20 %.[20] Despite achieving remarkable efficiency, these materials are inherently unstable under humid environments because of their ionic nature.[21] Further, they contain the RoHS prohibited element lead.[22] A significant amount of effort has been expended towards the development of lead-free perovskites for PV applications but their efficiency is limited.[23] Although the latest research efforts are driven towards better solutions for the challenges in existing technologies, achieving cost-effective electricity from PV still demands identifying new materials with requisite optical properties.[24] Consequently, we have been investigating the optical properties of a series of material systems including $Cu_2FeSnS_4$, Cu-Sb-S, and SnGe in nanocrystalline form.[15,25–28] The design of quaternary $M^{I}M_2^{II}M^{III}X_4^{VI}$ (I–$II_2$–III–$VI_4$) chalcogenides, produced by cation cross-substitution between ternary I–III–$VI_2$ and binary II–VI compounds, offers an attractive route for exploring novel materials.[29] We have recently succeeded in synthesizing a new family of quaternary semiconductors $Cu_2ZnMS_{4-x}$ and $CuZn_2MS_4$ (M = Al, Ga, In) in the form of wurtzite and stannite phase nanocrystals.[30] These materials have a direct band gap in the visible wavelength region combined with a high absorption cross-section.

Similar to the above, the $M^{I}M^{III}M^{IV}X_4^{VI}$ (I-III-IV-$VI_4$) chalcogenides are normal valence compounds which satisfy the tetrahedral bond rule, i.e., four valence electrons per atom including one cation vacancy.[31,32] Hence these quaternary materials can potentially be stabilized as wurtzite and zinc blende type phases (adamantine structures) with all atoms in tetrahedral positions.[33] Additionally, spinel-related structures, where the metal cations are tetrahedrally and/or octahedrally coordinated, can be realized.[34] Indeed, synthesis of spinel-related single crystals of $CuM^{III}SnS_4$ ($M^{III}$ = Al, Ga, In) was reported in the late 70's by high temperature chemical vapor transport (CVT) method using $AlCl_3/I_2$ as transport agents.[35,34] Bulk $CuInSnS_4$ crystallizes in the cubic spinel structure belonging to the $LiAlTiO_4$ family, whereas $CuGaSnS_4$ crystallizes in the orthorhombic

[a] UbiQD, Inc, 134 Eastgate Dr. Los Alamos, NM-87544. karthik@ubiqd.com
[b] Department of Chemistry & Biochemistry, The University of Alabama, Tuscaloosa, Al-35487
[c] Center for Materials for Information Technology, The University of Alabama, Tuscaloosa, AL-35487. agupta@mint.ua.edu
Electronic Supplementary Information (ESI) available: [details of any supplementary information available should be included here]. See DOI: 10.1039/x0xx00000x

structure.[36] $CuInSnS_4$ was determined to have an optical band gap of 1.1 eV, very close to the silicon indirect band gap.[37] Apart from preliminary studies of the spinel phase, these compounds have not been investigated in any other crystalline form.[38]

Herein, we report the synthesis and optical studies of wurtzite and defect chalcopyrite phases of $CuMSnS_4$ (M = In or Ga) nanocrystals (NCs) along with their photoelectric properties.

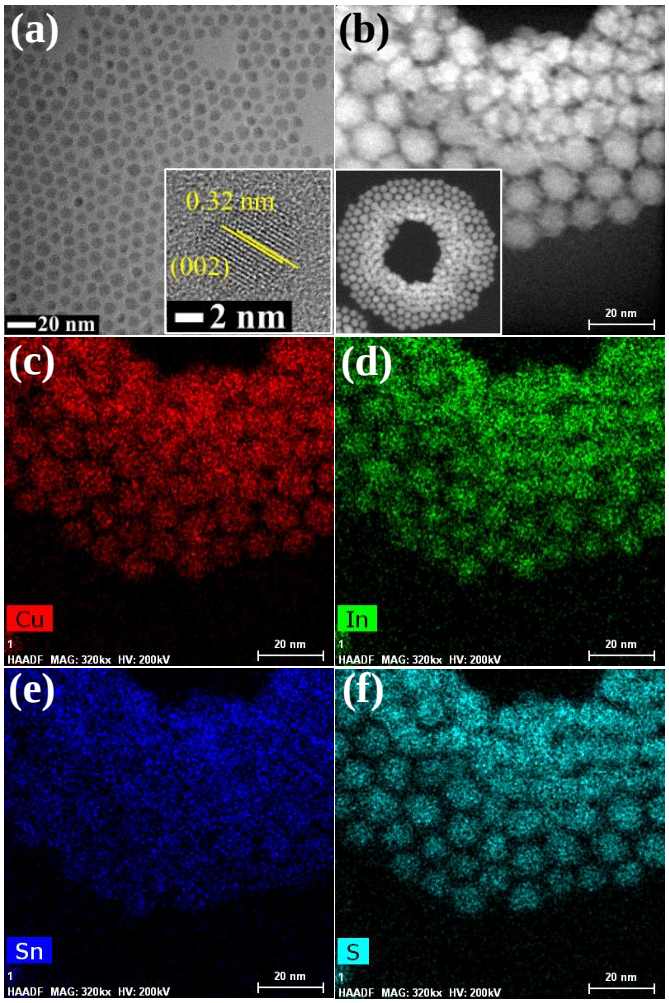


**Fig 1.** (a) TEM image of wurtzite phase $CuInSnS_4$ nanocrystals (inset: corresponding high-resolution TEM image). (b) High angle annular dark field (HAADF) images (inset: low magnification HAADF image. (c)-(f) STEM-EDX elemental mapping images of Cu, In, Sn and S.

The quaternary chalcogenides nanocrystals were synthesized using a colloidal hot-injection method. For the synthesis of wurtzite phase $CuMSnS_4$ (M = In or Ga) NCs a 1:1:1 ratio of acetylacetonate complexes of copper (II), indium (III) or gallium (III) and tetrahydrofuran adduct of tin (IV) chloride were dispersed in oleylamine and deaerated at room temperature for 15-30 min. The dispersion was heated to 150 °C in $N_2$ atmosphere and a mixture of *n*-dodecanethiol (*n*-DDT, 1 mL) and *tert*-dodecanethiol (*t*-DDT, 1 mL) was rapidly introduced into the reaction mixture at that temperature. The entire mixture was then heated to 210-215 °C and maintained at this temperature for 10 to 30 min. A similar synthesis procedure was followed for obtaining the defect chalcopyrite phase of $CuMSnS_4$ (M = In or Ga) NCs, but using sulfur dissolved in oleylamine as the sulfur source. For the structural determination and optical properties analysis, NCs sizes were sorted by selective precipitation method and the final precipitate fraction was chosen for the analysis.

The above one-pot synthesis approaches yield narrowly dispersed spherical shape wurtzite and pseudospherical (Fig 1a) defect chalcopyrite phase NCs with an average diameter of 10 ± 2 nm and 10 ± 2.5 nm, respectively, as imaged using transmission electron microscopy (TEM). The average size of the NCs estimated from TEM images is further corroborated using Small Angle X-ray Scattering analysis, as shown in Fig S1 & S2. High-resolution TEM images exhibit lattice fringes confirming the highly crystalline nature of NCs ( Fig 1a inset & FigS3). The average distance between the lattice fringes is estimated to be 0.32 nm for $CuInSnS_4$ NCs and 0.314 nm for $CuGaSnS_4$, matching with the (002) lattice planes of the wurtzite phase. Similarly, the lattice distance values measured from HRTEM images of defect chalcopyrite phase $CuInSnS_4$ and $CuGaSnS_4$ NCs are found to be 0.32 nm and 0.31 nm, respectively, corresponding to the (112) planes. The uniform distribution of elements throughout the interior of nanocrystals is established by High Angle Annular Dark Field (HAADF) imaging combined with 2D EDX elemental mapping. Typical images of wurtzite $CuInSnS_4$ NCs are shown in Fig 1(c-f), which show the homogeneous distribution of Cu, In, Sn and S over the entire NCs. A similar elemental homogeneity is observed for wurtzite $CuGaSnS_4$ and defect chalcopyrite $CuMSnS_4$ (M = In or Ga) NCs (Fig S4, S5 & S6). Further, the elemental composition estimated from EDX analysis of both phases of $CuMSnS_4$ (M =In or Ga) NCs indicate the total metal to sulfur atomic ratio to be close to 1:1 (Table S1), suggesting possible sulfur deficiency. Chalcogenide materials are known to accommodate large compositional variations, particularly anion non-stoichiometry.[36]

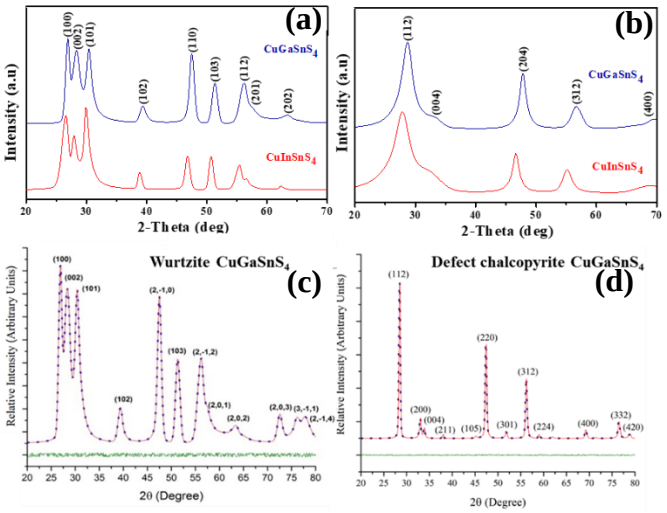


**Fig 2.** XRD patterns of (a) wurtzite and (b) defect chalcopyrite phases of $CuInSnS_4$ and $CuGaSnS_4$ nanocrystals. XRD pattern of (c) wurtzite and (d) defect chalcopyrite (annealed sample) $CuGaSnS_4$ nanocrystals along with Rietveld fittings.

In the bulk, $CuInSnS_4$ is reported to crystallize in the spinel cubic structure and $CuGaSnS_4$ is in the orthogonal structure with vacancy in the cation site.[37] However, in nanocrystalline form they crystallize as wurtzite and defect chalcopyrite phases. Fig. 2 shows powder X-ray diffraction (XRD) patterns confirming the pure wurtzite and defect chalcopyrite phases of $CuMSnS_4$ (M = In or Ga) NCs. There is no report for solution-based synthesis of $CuInSnS_4$ and $CuGaSnS_4$ in any structural form; especially it is unprecedented for these materials to be observed in wurtzite and defect chalcopyrite forms.

Therefore, XRD patterns of the NCs are fitted using Rietveld refinement method. The Rietveld fits of the experimental XRD patterns show good match for both phases. The experimental peaks can be indexed to the (100), (002), (101), (102), (110), (103), (112), and (201) planes of pure wurtzite phase and (112), (004), (204), (312) and (400) planes of defect chalcopyrite phase, respectively. The lattice parameter values (*a*) and (*c*) determined from the Rietveld fitting for wurtzite and defect chalcopyrite phases of $CuInSnS_4$ and $CuGaSnS_4$ are given in Table S2. Based on a comparison of XRD peaks and lattice parameter values, it is apparent that the NCs are devoid of any secondary impurity phases. In general, the wurtzite phase of ternary chalcogenides is a cation-disordered metastable phase formed at lower reaction temperatures, while the cubic spinel phase is expected at higher temperatures. In an attempt to isolate the spinel phase of $CuInSnS_4$, we have annealed the hexagonal phase NCs at 500 °C under $N_2$ atmosphere. The resulting material is found to be the defect chalcopyrite phase instead of cubic spinel as determined from X-ray diffraction measurements.

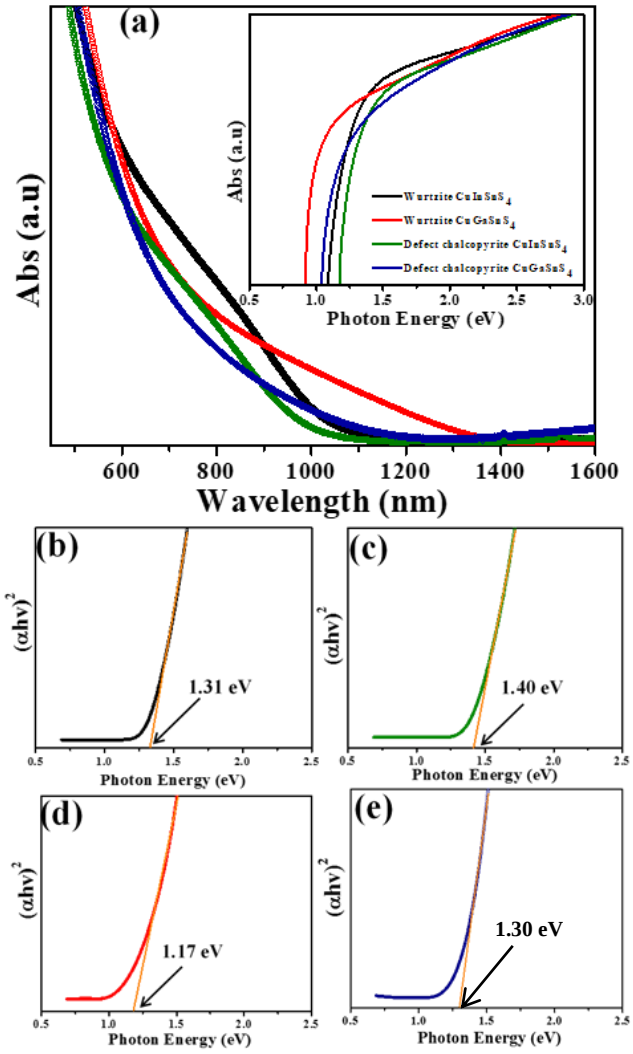


**Fig 3.** (a) Absorption spectra of wurtzite and defect chalcopyrite phase $CuInSnS_4$ and $CuGaSnS_4$ nanocrystals (Inset: absorption spectra in log scale). Tauc plots of (b) wurtzite phase $CuInSnS_4$, (c) defect chalcopyrite phase $CuInSnS_4$, (d) Wurtzite phase $CuGaSnS_4$, and (e) defect chalcopyrite phase $CuInSnS_4$ nanocrystals

To determine the oxidation states of the elements on the surface of the NCs, we have carried out X-ray photoelectron spectroscopy (XPS) measurements on wurtzite phase $CuInSnS_4$. The survey scan XPS spectrum exhibits peaks corresponding to Cu, In, Sn and S elements, along with C but absence of oxygen or any other impurities, which is consistent with EDX elemental data. The $Cu_{2p}$ core-spectrum shows two major peaks at 931.4 eV ($2p_{3/2}$) and 951.2 eV ($2p_{1/2}$) with a peak splitting of 20.0 eV, indicative of the monovalent state of Cu. The $In_{3d}$ spectrum shows contributions from $3d_{5/2}$ and $3d_{3/2}$ at 444.6 eV and 452.2 eV, respectively, indicating a spin-orbit splitting of 7.6 eV, characteristic of In(III). The Sn $3d_{5/2}$ and $3d_{3/2}$ peaks are fitted with Gaussian components at 486 eV and 494 eV, which can be assigned to Sn(IV). The sulfur spectrum with peaks at binding energies 162.2 eV ($2p_{3/2}$) and 163.2 eV ($2p_{1/2}$) and a doublet separation of 1.1 eV can be attributed to the presence of $S^{2-}$ (Fig S8). The oxidation states of elements determined from the XPS analysis further corroborate the $CuMSnS_4$ (M = In or Ga) composition.

Optical properties of the new class of chalcogenide materials have been investigated using ultraviolet-visible spectroscopy (UV-vis) measurements on well-dispersed NC solutions in hexane (Fig 3a). The absorption spectra of $CuMSnS_4$ (M = In or Ga) NCs exhibit absorption over a wide wavelength range, with strong absorption in the visible region and a drop off in the intensity at longer wavelengths. To estimate the band gap of the synthesized NCs, the commonly utilized Tauc method is used. The direct optical band gaps ($E_{g,opt}$) are determined from the absorbance spectra onset through extrapolating the linear portion of the $(Ah\nu)^2$ versus $h\nu$ ($A$=absorbance, $h$=Planck's constant, and $\nu$=frequency) plot in the band edge region (Fig 3 (b)-(e)). The estimated band gaps of wurtzite and defect chalcopyrite phases of $CuMSnS_4$ (M = In or Ga) NCs are between 1.15 and 1.4 eV, with the former having a wider gap. The band gaps of both wurtzite and defect chalcopyrite phases of $CuInSnS_4$ NCs are close to that reported for spinel phase $CuInSnS_4$ and comparable to silicon, CIGS, GaAs and CdTe absorbers.[38-41]

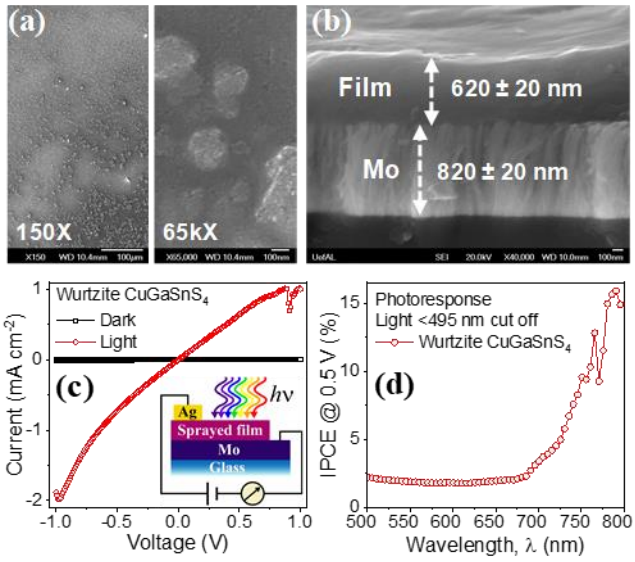


**Fig 4**. SEM images of (a) top with different magnifications, and (b) cross-section view of ~600 nm thick Wurtzite $CuGaSnS_4$ thin film fabricated on Mo-coated glass substrate using spray-deposition from Wurtzite $CuGaSnS_4$ NCs and annealed in $N_2$ at 375 °C. (c) Current–Voltage (*J-V*) characteristics of Wurtzite $CuGaSnS_4$ thin film device under white light illumination at 100 mW $cm^{-2}$ (Inset: schematic of device prepared for *J-V* measurement). (d) Spectral response of a Wurtzite $CuGaSnS_4$ thin film device at 0.5 V (Light before 495 nm was cut off using GG495 filter)

To evaluate the suitability of $CuMSnS_4$ (M = In or Ga) NCs for solar cell application, we have carried out photocurrent measurements on spray coated and annealed nanocrystalline films sandwiched between Mo-coated soda-lime glass substrate and silver top contact layer (Fig 4(a&b)). The *J-V* characteristics of the films showed a significant photoconductivity with non-rectifying behaviour from all four NCs under 1 Sun white light illumination condition at room temperature. The representative J-V curve for wurtzite $CuGaSnS_4$ NCs films is shown in Fig 4(c). Further, to test wavelength-dependent photoconductivity, we have illuminated the NCs films at wavelengths between 500 and 800 nm. Fig 4d shows the incident photon-to-current conversion efficiency (IPCE) plot for wurtzite $CuGaSnS_4$ thin film that clearly exhibits higher spectral response at wavelengths higher than 700 nm and reaching maximum efficiency of ~16% at 800 nm, closer to the bandgap. The measured IPCE values for other phases of NCs are found to be between 4 and 7%.

In conclusion, we have developed a facile synthetic approach to produce colloidal $CuMSnS_4$ (M = In or Ga) NCs. The sizes of the NCs range from 8-14 nm with narrow size distributions. The NCs are synthesized by hot-injection method, wherein a mixture of thiols is injected into a reaction vessel containing a solution of the metal precursors at an elevated temperature. The use of thiols as a sulfur source yields wurtzite phase NCs, whereas sulfur in oleylamine solution produces defect chalcopyrite phase NCs. Additionally, wurtzite phase NCs can be converted to the defect chalcopyrite phase by annealing at 400-450 °C. As-synthesized wurtzite and defect chalcopyrite NCs exhibit pseudo spherical to spherical morphology. We have observed a homogeneous distribution of elements in NCs from HAADF and STEM-EDX elemental mapping images. Absorption measurements confirm that these compounds are direct band gap semiconductors possessing energy gaps between 1.15 eV and 1.40 eV. Our studies suggest that $CuMSnS_4$ (M = In or Ga) materials are potential cost-effective and efficient solar energy absorbers as they possess suitable optical and photocurrent properties.

## Conflicts of interest

"There are no conflicts to declare".

The National Science Foundation under Grant No. CHE-1508259 supported the work at the University of Alabama. This work was also performed, in part, at the Center for Integrated Nanotechnologies, an Office of Science User Facility operated for the U.S. Department of Energy (DOE) Office of Science by Los Alamos National Laboratory (Contract DE-AC52-06NA25396).

## Notes and references

(1) N. Panwar, S. Kaushik, S. Kothari, *Renew. Sustain. Energy Rev,* 2011, **15**, 1513.
(2) M. Z. Jacobson, M. A. Delucchi, *Energy Policy,* 2011, **39**, 1154.
(3) A. K. Pandey, N. ARahim, M. Hasanuzzaman, P. Pant, V. V. Tyagi, *Green Technologies and Environmental Sustainability*, 2017, 157–178.
(4) T. M. Razykov, C. S. Ferekides, D. Morel, E. Stefanakos, H. S.Ullal, H. M. Upadhyaya, *Sol. Energy,* 2011, **85**, 1580.
(5) K. Zweibel, J. Mason, V. Fthenakis, *Sci. Am.* 2008, **289**, 64.
(6) A. V. Shah, H. Schade, M. Vanecek, J. Meier, et. al., *Prog. Photovoltaics Res. Appl,* 2004, **12**, 113.
(7) J. D. Major, R. E. Treharne, L. J. Phillips, K. Durose, *Nature,* 2014, **511**, 334.
(8) M. Yamaguchi, T. Takamoto, K. Araki, N. Ekins-Daukes, *Sol. Energy,* 2005, **79**, 78.
(9) K. Ramanathan, M. A. Contreras, C. L. Perkins, S. Asher, et.el., *Prog. Photovoltaics Res. Appl.* 2003, **11**, 225.
(10) L. Grandell, M. Höök, *Sustain,* 2015, **7**, 11818.
(11) K. Zweibel, *Sol. Energy Mater. Sol. Cells,* 2000, **63** (4), 375.
(12) D. Bonnet, *Thin Solid Films,* 2000, **361**, 547.
(13) K. Ramasamy, M. A. Malik, N. Revaprasadu, P. O'Brien, *Chem. Mater.* 2013, **25** (18), 3551.
(14) G. M. Ford, Q. Guo, R. Agrawal, H. W. Hillhouse, *Chem. Mater,* 2011, **23**(10), 2626.
(15) K. Ramasamy, P. G. Kotula, A. F. Fidler, M. T. Brumbach, J. M. Pietryga, S. A. Ivanov, *Chem. Mater,* 2015, **27**, 4640.
(16) K. Ramasamy, M. A. Malik, P. O'Brien, *Chem. Sci.* 2011, **2**(6), 1170.
(17) A. A. Yaroshevsky, *Geochemistry Int.* 2006, **44**, 48.
(18) K. Ramasamy, M. A. Malik, P. O'Brien, *Chem. Commun.* 2012, **48**, 5703.
(19) W. Wang, M. T. Winkler, O. Gunawan, T. Gokmen, T. K. Todorov, Y. Zhu, D. B. Mitzi, *Adv. Energy Mater,* 2014, **4** (7), 1301465.
(20) S. Shin, E. J. Yeom, W. S. Yang, S. Hur, M. G. Kim, J. Im, J. Seo, J. H. Noh, S. Seok, *Science,* 2017, **356**, 167.
(21) J. M. Frost, K. T. Butler, F. Brivio, C. H. Henddon, M. V. Schilfgaarde, A. Walsh, *Nano Lett.* 2014, **14**, 2584.
(22) H. Tang, S. He, C. Peng, *Nanoscale Res. Lett.* 2017, **12** (1), 410.
(23) Z. Shi, J. Guo, Y. Chen, Q. Li, Y. Pan, H. Zhang, Y. Xia, W. Huang, *Adv. Mater,* 2017, **29** (16), 1605005.
(24) X. G. Zhao, J. Yang, Y. Fu, D. Yang, Q. Xu, L. Yu, S. H. Wei, L. Zhang, *J. Am. Chem. Soc,* 2017, **139**, 2630.
(25) K. Ramasamy, H. Sims, W. H. Butler, A. Gupta, *Chem. Mater* 2014, **26**, 2891.
(26) K. Ramasamy, B. Tien, P.S. Archana, A. Gupta, *Mater. Lett.* 2014, **124**, 227.
(27) K. Ramasamy, H. Sims, W. H. Butler, A. Gupta, *J. Am. Chem. Soc.* 2014, **136**, 1587.
(28) X. Zhang, N. Bao, K. Ramasamy, Y. H. A. Wang, Y. Wang, B. Lin, A. Gupta, *Chem. Commun.* 2012, **48** (41), 4956.
(29) A. Walsh, S. Wei, S. Chen, X. Gong, *IEEE Photovolt. Spec. Conf.* 2009, 1875.
(30) A. Ghosh, S. Palchoudhury, R. Thangavel, Z. Zhou, N. Naghibolashrafi, K. Ramasamy, A. Gupta, *Chem. Commun,* 2016, **52** (2), 264.
(31) D. K. Ghosh, P. S. Ghosh, L. K. Samanta, *Phys. Rev. B,* 1990, **41** (8), 5126.
(32) H. Matsushita, T. Maeda, A. Katsui, T. Takizawa, *J. Cryst. Growth,* 2000, **208**, 416.
(33) H. Matsushita, A. Katsui, *J. Phys. Chem. Solids,* 2005, **66** (11), 1933.
(34) G. Concas, L. Garbato, F. Ledda, *Prog. Cryst. Growth Charact. Mater,* 1993, **25**, 39.
(35) T. Ohachi, B. R. Pamplin, *J. Cryst. Growth,* 1977, **42**(C), 598.
(36) C. Steinhagen, M. G. Panthani, V. Akhavan, B. Goodfellow, B. Koo, B. A. Korgel, *J. Am. Chem. Soc*., 2009, **131**, 12554; U. V. Ghorpade, M. P. Suryawanshi, S. W. Shin, I. Kim, S. K. Ahn, J. H. Yun, C. Jeong, S. S. Kolekar, J. H. Kim, *Chem. Mater*., 2016, **28**, 3308.
(37) L. Garbato, *J. Cryst. Growth,* 1991, **114**(3), 299.
(38) B. R. Pamplin, R. S. Feigelson, *Mater. Res. Bull,* 1979, **14** (1), 1.
(39) C. Yang, M. Qin, Y. Wang, D. Wan, F. Huang, J. Lin, *Sci. Rep*, 2013, **3**, 1286: M. Zribi, M. B. Rabeh, R. Brini, M. Kanzari, R. Rezig, *Thin Solid Films*, 2006, **511-512**, 125: M. M. Han, X. L. Zhang, Z. Zeng, *RSC Adv*., 2016, **6**, 110511.
(40) K. Tanabe, D. Guimard, D. Bordel, Y. Arakawa, *Appl. Phys. Lett.* 2012, **100** (19), 193905.
(41) G. D. Cody, B. G. Brooks, B. Abeles, *Sol. Energy Mater,* 1982, **8**, 231.

 

## Graphical Abstract

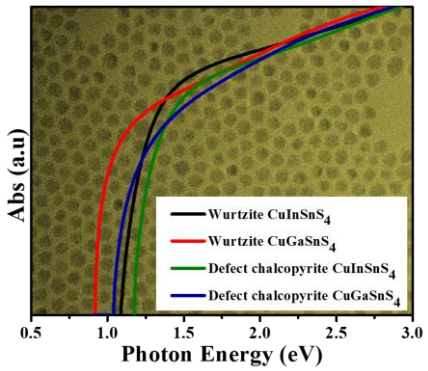


**Nanocrystals of wurtzite and defect chalcopyrite phases of $CuMSnS_4$ (M = In or Ga) have been synthesized that exhibit strong visible light absoprtion with band gap between 1.15 and 1.40 eV.**